Evaluating the Efficacy of Pulse Transit Time between Palm and Forehead in Blood Pressure Estimation

Chuchu Qiu
The Hong Kong University of Science and Technology
Hong Kong, China
cqiuac@connect.ust.hk

Jing Wei Chin
PanopticAI Limited
Hong Kong, China
jwchin@connect.ust.hk

Tsz Tai Chan
PanopticAI Limited
Hong Kong, China
ttchanac@connect.ust.hk

Kwan Long Wong
PanopticAI Limited
Hong Kong, China
kylewong@panoptic.ai

Richard Hau Yue So
The Hong Kong University of Science and Technology
Hong Kong, China
rhyso@ust.hk

Abstract

Traditional cuff-based blood pressure (BP) measurement techniques, though widely employed, require a cuff that must be fitted and inflated and thus are limited by convenience issues. In contrast, contactless BP monitoring solutions offer a promising alternative. This study explored pulse transit time (PTT) as a feature for accurate BP monitoring using remote photoplethysmography (rPPG). The investigation examined the order of PTT (PTT Order) between the palm and forehead and their impacts on the accuracy of BP estimation. Our findings showed variation in the dominant order between the two sites among the subjects. Nevertheless, the inverse of mean PTT extracted from the two sites in dominant order (PTT Dominant Order) consistently showed a higher linear correlation with systolic blood pressure (SBP). The mean and standard deviation of R-squared derived from the inverse of mean PTT with the dominant order and SBP among the 16 subjects were 0.81 ± 0.13. Additionally, subgroup analysis identified significant differences in SBP across gender and exercise status. Furthermore, our data revealed a hysteresis phenomenon in 25% of the subjects, characterized by SBP returning to baseline levels during post-exercise resting while heart rate (HR) remained persistently elevated.

CCS Concepts

• **Theory of computation** → *Theory and algorithms for application domains.*

Keywords

Pulse Transit Time (PTT), PTT Dominant Order, Blood Pressure(BP) Estimation, Remote Photoplethysmography (rPPG)

ACM Reference Format:
Chuchu Qiu, Jing Wei Chin, Tsz Tai Chan, Kwan Long Wong, and Richard Hau Yue So. 2025. Evaluating the Efficacy of Pulse Transit Time between Palm and Forehead in Blood Pressure Estimation. In *Proceedings of the 27th International Conference on Multimodal Interaction (ICMI '25), October 13–17, 2025, Canberra, ACT, Australia.* ACM, New York, NY, USA, 9 pages. https://doi.org/10.1145/3716553.3750789

ICMI '25, Canberra, ACT, Australia

ACM ISBN 979-8-4007-1499-3/25/10
https://doi.org/10.1145/3716553.3750789

1 Introduction

Cardiovascular diseases (CVDs) represent a significant and extremely serious global health issue, accounting for an estimated 17.9 million lives each year [3]. Therefore, hypertension is recognized as a major risk factor that considerably increases the likelihood of developing CVD [14]. According to recent statistics from the World Health Organization (WHO), published in March 2023 [1], approximately 1.28 billion adults aged 30 to 79 years worldwide are affected by hypertension. Notably, an estimated 46% of these individuals are unaware of their hypertensive status, indicating a critical gap in both diagnosis and management. Consequently, regular monitoring of blood pressure (BP) and timely intervention are essential for reducing the risk of CVD. Traditional cuff-based BP measurements have been widely utilized; however, they present limitations in terms of convenience [7], such as the use of a cuff that must be properly fitted and inflated. An alternative approach involves estimating BP through pulse transit time (PTT) using photoplethysmography (PPG) and electrocardiogram (ECG) signals [5, 9, 19], which offers increased convenience and the potential for continuous monitoring without the need for cuffs. Nevertheless, this contact-based method requires specific devices to be worn, such as smartwatches. In contrast, remote photoplethysmography (rPPG) has been developed with more accessible devices such as smartphones to enhance its advantages by providing a contactless and more user-friendly experience.

Despite its benefits, the existing literature reveals inconsistencies regarding the reliability of the PTT Order between the palm and the forehead. This raises the question of whether the PTT should be expressed from the palm to the forehead or vice versa, which necessitates further investigation [8, 17, 21]. Consequently, the primary research question of this study is: Is the use of the palm-forehead configuration advisable for estimating blood pressure?

The present study is structured around three primary objectives: (i) To investigate the PTT Order between the palm and the forehead as specific arterial sites. (ii) To analyze the implications of this PTT Order on BP estimation, with a particular focus on its effects

on accuracy. (iii) To conduct a subgroup analysis across various demographic groups.

This study provides a comprehensive analysis of the effects of PTT Order on BP estimation within a controlled laboratory setting. The key contributions of this research are summarized as follows:

(1) Subject variability in the dominant order of PTT: the dominant order of PTT (PTT Dominant Order) varied between palm and forehead across subjects, suggesting the necessity of considering individual differences when utilizing these sites for BP estimation.
(2) Enhanced Predictive Correlation: The R-squared between the inverse of the mean PTT with the dominant order and systolic blood pressure (SBP) was consistently higher than the other order of PTT, thus reinforcing its potential for accurate BP estimation.
(3) Demographic and Physiological Influences: There were no significant differences in SBP estimation error across both gender and exercise status groups. Besides, the hysteresis phenomenon was observed between heart rate (HR) and SBP.

2 Related Works

To enhance non-invasive and convenient BP monitoring, researchers have increasingly focused on contactless estimation methods. Recent advancements in this field primarily address two strategies: waveform feature analysis and PTT measurements. Waveform feature analysis has focused on evaluating the shape and characteristics of rPPG to estimate BP through various methodologies. Li et al. [20] extracted time-domain features like pulse height and duration, energy-domain metrics, and physiological parameters such as HR for machine learning models. However, the rationale behind their feature selection remained unclear. Wu et al. [27] incorporated waveform features and physiological signals into their model involving a substantial dataset with 1,143 subjects. However, the model's effectiveness was hindered by poor signal quality. Cheng et al. [6] demonstrated that a transfer learning approach could surpass the performance of state-of-the-art models, even with a much smaller dataset of 17 subjects.

In contrast, PTT-based methods have utilized the Moens-Korteweg (M-K) equation, where the inverse of PTT exhibited a linear relationship with BP [26]. Traditionally, PTT measurements employed ECG R-waves and peripheral PPG signals, such as those from the fingertip [5, 9, 19]. However, recent research on contactless methods has explored alternative body regions for more convenient use. Numerous studies have examined and evaluated the regression relationship between PTT and BP using rPPG in various areas, including the forehead, palm, right cheek, wrist, and ankle [8, 16–18, 21, 22, 28], highlighting its potential for contactless monitoring techniques. Among the frequently explored sites for PTT measurement, the combination of the palm and forehead was commonly investigated [8, 17, 21, 22, 28].

However, the temporal relationship between these two sites, specifically the PTT Order, has not been extensively studied in the literature. Fan et al. [8] and Secerbegovic et al. [21] assumed that forehead pulses precede palm arrivals, dismissing reverse cases as motion artifacts. Conversely, Lu et al. [17] reported bidirectional pulse transit times (both positive and negative values) in face-to-arm measurements across subjects, challenging the common assumption of a universal forehead-first pulse arrival pattern used in previous studies. Given these discrepancies, our paper aimed to investigate the order of PTT between the palm and forehead and its implications for accurate BP estimation.

3 Methods

3.1 Experimental Setup

To facilitate our study, we developed an experimental setup, as depicted in Figure 1. This configuration included a camera system based on an iPad Air 5th generation, which operated at a frame rate of 60 frames per second with a 1280 x 720 pixels resolution. For reference BP measurements, we utilized a Food and Drug Administration (FDA) approved automated oscillometric BP monitor (Uscom BP+). To reduce potential motion artifacts, we employed a fixed headrest and a handrest to assist subjects in maintaining a stationary position throughout the recording process. The camera was positioned 40 cm from the subject's face, with illumination levels maintained at approximately 1000 lux on both facial and palm areas, measured with luminometers (UNI-T UT382).

Furthermore, we included an FDA-approved pulse oximeter (MightySat® Rx Fingertip Pulse Oximeter) to measure HR during exercise, as well as an FDA-approved Body Composition Monitor (Tanita BC-545N) to assess subject weight. Ambient temperature and humidity levels were recorded prior to the commencement of the study using an environmental sensor (UNI-T UT332). The ambient temperature was measured at 22.82 ± 0.42 °C (mean ± standard deviation), while the humidity level was recorded at 43.02 ± 9.48%.

3.2 Experiment Protocol

The experimental procedure lasted approximately 60 minutes and was divided into three periods: pre-exercise, during exercise, and post-exercise, as shown in Figure 2. Data collection occurred exclusively during the pre-exercise and post-exercise periods when subjects were resting and stationary with their palms raised. Both the pre-exercise and post-exercise periods lasted around 25 minutes, and both periods were identical. The pre-exercise period included eight sessions, each taking about 3 minutes. Each session began with a 1-minute video recording, during which the reference BP measurement was started concurrently, taking approximately 1.5 minutes to complete, followed by 1.5 minutes of resting.

During the exercise period, subjects engaged in a high intensity pedaling exercise lasting a minimum of 5 minutes, with a pulse oximeter affixed to the right index finger to monitor HR. The exercise continued until subjects exceeded 5 minutes of pedaling and reached 70% of their maximum HR, maintaining this level or above for at least 10 seconds, calculated using the formula: 70% of (220 - Age) [2, 24]. In addition, subjects' weight and height were recorded before data recording began.

3.3 Data Information

We collected a dataset consisting of 16 healthy subjects in a controlled laboratory environment. A sample video frame is shown in Figure 3. Demographic and medical information for each subject was documented, including gender (10 females and 6 males),

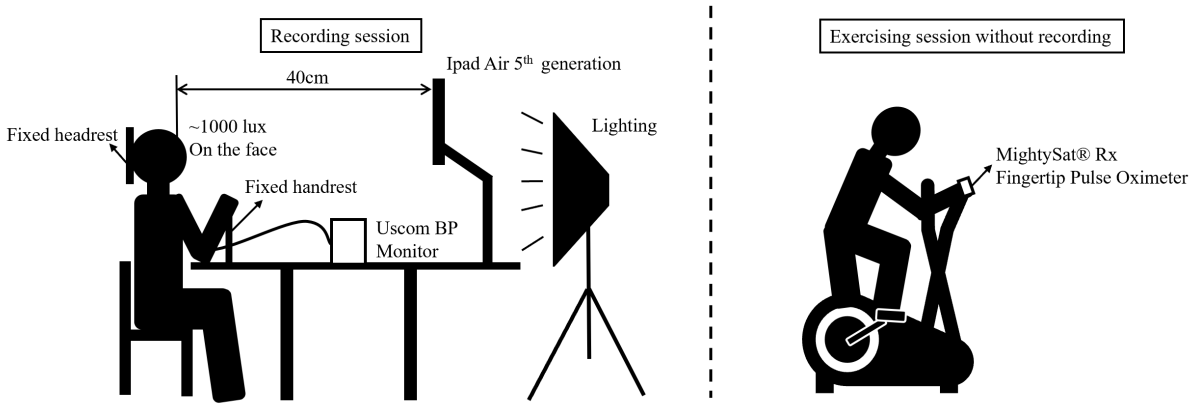

Figure 1: Experimental Setup. Data for analysis was collected solely during the recording session, with the subject remaining seated and their right palm raised.

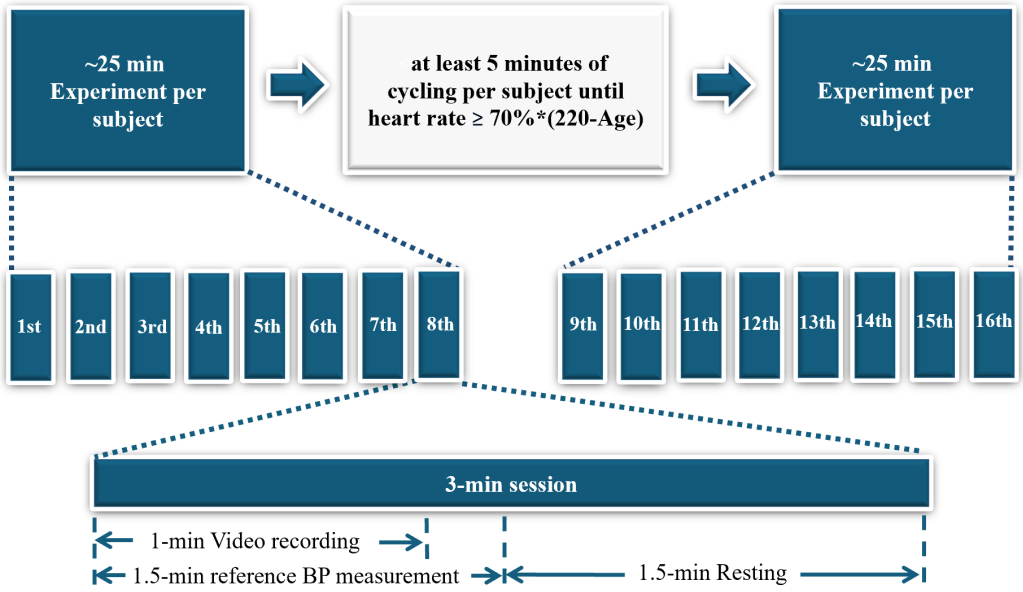

Figure 2: Experimental Protocol

age (25.25 ± 4.22 *years*), height (167.31 ± 8.61 *cm*), weight (59.49 ± 8.58 *kg*), Body Max Index (BMI) (21.17 ± 1.85 $kg * m^{-2}$), ethnicity (all subjects were of Asian descent) and smoking history. Subjects who wore makeup or other topical facial products were excluded from the study. Vulnerable individuals unable to provide informed consent, such as those with mental disabilities, were also excluded from the study.

3.4 Data Processing

The data processing pipeline involved six key steps, as illustrated in Figure 4. The initial four steps included regions of interest (ROI) selection, obtaining the mean RGB signal, extracting the raw rPPG signal, and obtaining the filtered rPPG signal, as shown in panels (a) to (d) of Figure 4. The subsequent steps involved calculating the beat-by-beat PTT and mean PTT values, as well as performing a regression analysis between the inverse of the mean PTT and SBP, as shown in panels (e) and (f) of Figure 4.

3.4.1 Obtaining filtered rPPG signal. The ROIs on the palm and forehead, as illustrated in Figure 4 (a), were manually selected for analysis. The ROI sizes were determined by calculating the intersection of all manually labeled regions across 16 subjects, resulting in fixed dimensions: the ROI on the forehead was 108 x 23 pixels, and the ROI on the palm was 92 x 74 pixels. We averaged the color

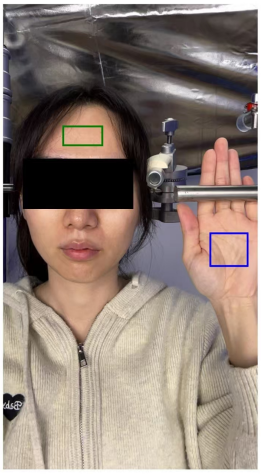

Figure 3: Sample Video Frame. This sample showed an anonymized volunteer with designated ROIs clearly highlighted. The green rectangle indicated the targeted forehead area, while the blue rectangle delineated the palm region. These marked zones serve as the primary focal points for data acquisition and analysis within the context of this study.

intensities within the red, green, and blue channels, shown in Figure 4 (b), and extracted the raw rPPG signal from the green channel [25], shown in Figure 4 (c). Subsequently, a 4th order zero-phase shift band-pass filter was applied within the frequency range of 0.5 to 3 Hz, corresponding to HR limits of 30 to 180 beats per minute (bpm). This step effectively minimized extraneous noise and artifacts within the signal. The raw rPPG signal was then normalized and inverted to align its shape with that of a PPG signal [23], as demonstrated in Figure 4 (d).

3.4.2 Beat-by-beat PTT Calculation. Beat-by-beat PTT was defined as the peak-to-peak time delay between the palm and forehead, where the peak represented the foot of the waveform. Previous empirical studies had established that beat-by-beat PTT values between the palm and forehead typically ranged above zero and up to 167 milliseconds (ms) [22, 28], and consequently, beat-by-beat PTT values exceeding this threshold in this study were considered invalid. We defined two types of beat-by-beat PTT between the palm and forehead according to previous studies[8, 17, 21], shown in Equation 1 and Equation 2.

$$PTT_{PF} = t_F - t_P \tag{1}$$

$$PTT_{FP} = t_P - t_F \tag{2}$$

Where PTT_{PF} is denoted as the beat-by-beat PTT when the palm peak came faster than the forehead peak, PTT_{FP} denoted as the beat-by-beat PTT when the forehead peak came faster than the palm peak, t_F is denoted as the timestamp of the forehead peak and t_P is denoted as the timestamp of the palm peak.

3.4.3 Definition of PTT Order and PTT Dominant Order. The question of whether the palm or forehead should be considered the proximal location remained unresolved. To address this uncertainty, we introduced the concepts of "PTT Order" and "PTT Dominant Order."

The PTT Order referred to the order of two sites that demonstrate a greater number of PTT values from one site to the other within a 1-minute window. There were two possible scenarios for the PTT Order: $O_{PM->FH}$ and $O_{FH->PM}$. The condition $O_{PM->FH}$ indicates there were more instances where the palm signal arrived faster than the forehead signal within the 1-minute window (see Figure 5). Conversely, $O_{FH->PM}$ indicated that the forehead signal arrived faster than the palm signal more frequently within the same time frame (see Figure 6).

In contrast, the PTT Dominant Order signified the most frequently observed PTT Order throughout the entire experimental duration. Regarding the PTT Dominant Order, three scenarios were possible: one where the palm signal consistently preceded the forehead signal across all 16 sessions, denoted as $DO_{PM->FH}$; another where the forehead signal consistently came earlier than the palm, denoted as $DO_{FH->PM}$; and a final scenario where both conditions coexisted.

3.5 Regression analysis

According to the M-K equation [26], the inverse of PTT was linearly related to BP. To validate this relationship, a linear regression analysis was conducted between the inverse of the mean PTT and SBP, as illustrated in Figure 4 (f). The mean PTT was calculated by averaging the PTT values over a 1-minute window, representing the average of all beat-by-beat PTT values of the same type (see section 3.4.2) within that period. There were two types of mean PTT: $mean\_PTT_{PF}$ and $mean\_PTT_{FP}$. Each type was used separately to estimate SBP, allowing for a comprehensive evaluation of the relationship between the inverse of the mean PTT, denoted as $1/mean\_PTT$ and SBP.

3.6 Metrics

R-squared, denoted as R^2, quantifies the proportion of variance in the dependent variable that is predictable from the independent variable in a linear regression model. The equation for R^2, shown in Equation 3, is as follows: SBP_i represents the i_{th} reference SBP, $\widehat{SBP}_i$ represents the i_{th} estimated SBP, and $\overline{SBP}_i$ represents the mean of the 16 reference SBP.

$$R^2 = 1 - \frac{\sum(SBP_i - \widehat{SBP}_i)^2}{\sum(SBP_i - \overline{SBP})^2} \tag{3}$$

4 Results and Analysis

Following data processing, the raw and filtered PTT signals from the palm and forehead were obtained, as illustrated in Figure 7. Subfigures (a) and (b) presented the raw and filtered rPPG signals from the palm, respectively. Similarly, subfigures (c) and (d) displayed the raw and filtered rPPG signals from the forehead.

4.1 Assessment of PTT Dominant Order: Palm vs Forehead

A descriptive analysis was performed to determine the PTT Dominant Order by counting the occurrences of each PTT Order within a 1-minute window across 16 sessions, shown in Table 1. For the majority of subjects (10 out of 16), the dominant order was $DO_{PM->FH}$,

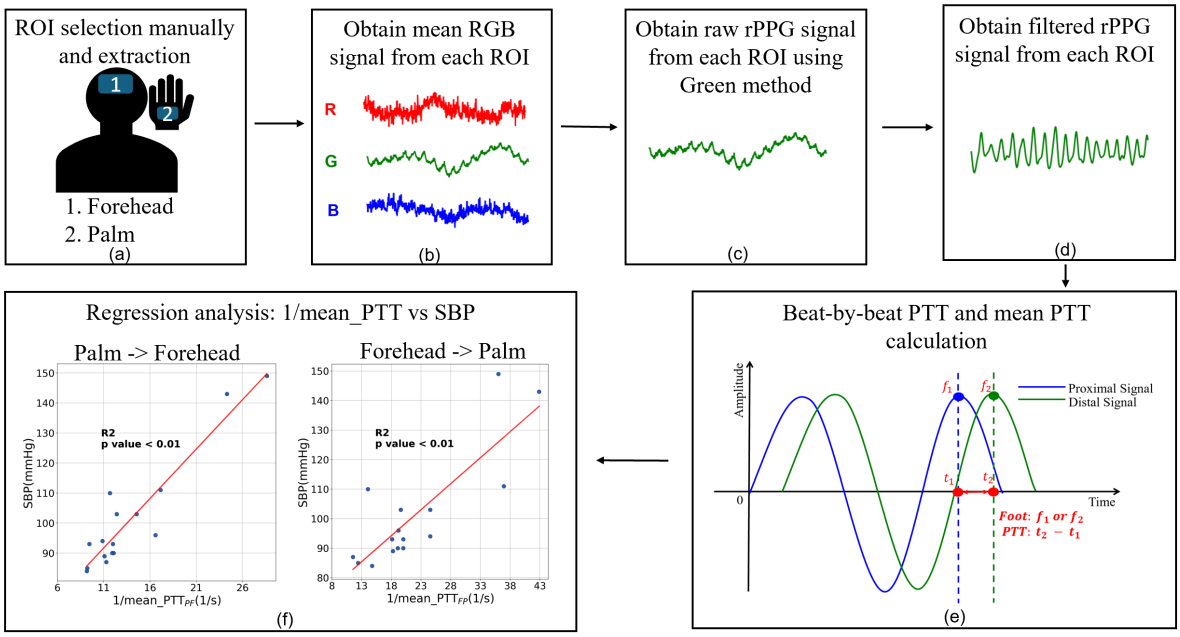

Figure 4: Data Processing Pipeline. The figure presented a flowchart outlining the methodology for estimating BP. This approach primarily aimed to calculate the mean PTT for each subject and to examine its correlation with SBP. The data processing pipeline involved six key steps. The initial four steps included manually selecting the ROIs, obtaining the mean RGB signal, extracting the raw rPPG signal, and filtering the rPPG signal, shown in panels (a) to (d) of the figure. Subsequently, the final steps included calculating the PTT values and conducting a regression analysis, shown in panels (e) to (f).

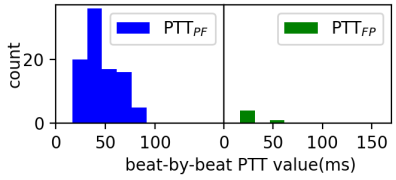

Figure 5: Sample of PTT Distribution from 9th session of Subject 4. The blue bar indicated PTT_{PF} where the palm signal arrived earlier than the forehead signal while the green bar represented cased PTT_{FP} where the forehead signal arrived earlier than the palm signal. The number of PTT_{PF} is larger than the number of PTT_{FP}, revealing that the PTT Order is $O_{PM->FH}$, which is the palm signal exhibited a faster arrival compared to the forehead signal in the 9th session of Subject 4.

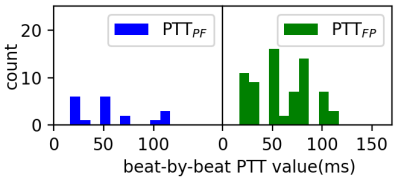

Figure 6: Sample of PTT Distribution from 10th session of Subject 10. The blue bar indicated PTT_{PF} where the palm signal arrived earlier than the forehead signal while the green bar represented cases PTT_{FP} where the forehead signal arrived earlier than the palm signal. The number of PTT_{FP} is larger than the number of PTT_{PF}, revealing that the PTT Order is $O_{FH->PM}$, meaning the forehead signal preceded the palm signal in the 10th session of Subject 10.

where all 16 windows in these subjects showed the palm signal preceding the forehead signal, with no instances of the reverse order. Five subjects exhibited a PTT Dominant Order labeled as "Both Exists," indicating the presence of windows where both PTT Order conditions—$O_{PM->FH}$ and $O_{FH->PM}$ were observed. Only one subject (Subject 10) demonstrated a dominant order of $O_{FH->PM}$, with all 16 windows reflecting this order and none showing the reverse. This analysis revealed a pronounced trend of $DO_{PM->FH}$ among the 16 subjects, with a few exceptions where both orders coexisted and $DO_{FH->PM}$ was observed.

Subsequently, we analyzed the distribution of the PTT Dominant Order. The results indicated that 62.5% of the subjects exhibited a dominant order where the palm signal arrived earlier than the forehead signal ($DO_{PM->FH}$). In contrast, only 6.25% of the subjects demonstrated a dominant order where the forehead signal arrived earlier than the palm signal ($DO_{FH->PM}$). The remaining 31.25% of the subjects exhibited instances where both scenarios occurred.

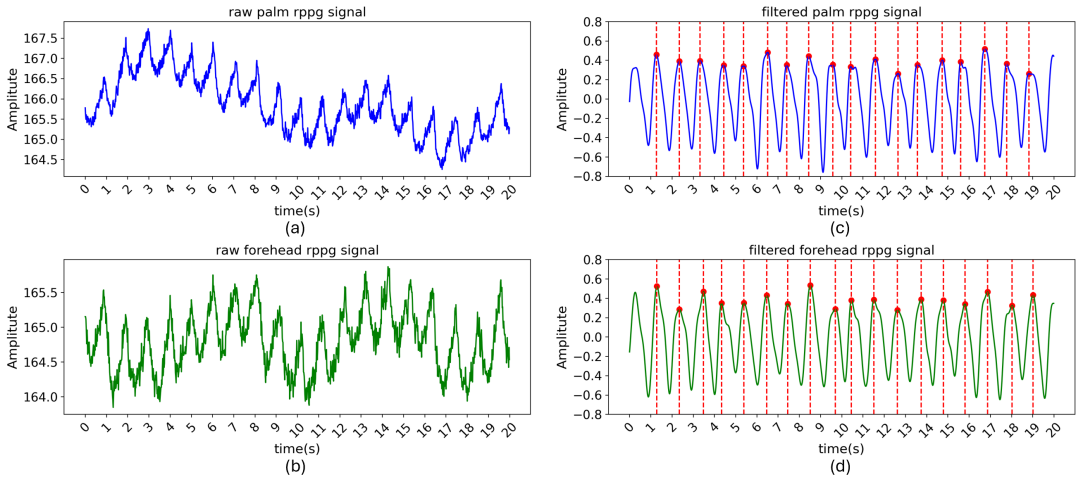

Figure 7: Processing of the raw rPPG signals from the Green Channel to generate filtered rPPG signals is illustrated. Panels (a) and (b) displayed the raw rPPG signal from the palm and forehead. Panels (c) and (d) depicted the corresponding filtered rPPG signal.

Although a majority of subjects exhibited earlier pulse arrival at the palm compared to the forehead, we observed a substantial subset demonstrating the reverse pattern. Further investigation is needed to determine whether this PTT Dominant Order has any impact on BP estimation.

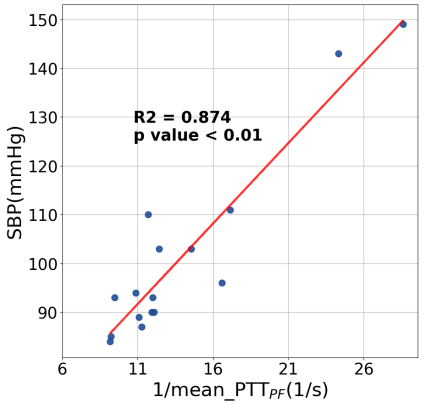

Figure 8: Linear Regression Results from Subject 4. The analysis of the inverse of $mean\_PTT_{PF}$ in relation to SBP yielded an R-squared = 0.874, with p-value <0.01, indicating a statistically significant correlation.

4.2 Effect of PTT Orders on BP Estimation: Dominant vs. Non-Dominant

To investigate the effects of PTT Dominant Order and PTT Non-Dominant Order on BP estimation, we conducted a regression analysis between the inverse of $mean\_PTT_{PF}$ and the inverse of $mean\_PTT_{FP}$ with SBP, as depicted in Figure 8 and Figure 9 respectively. These figures, derived from Subject 4, demonstrated a

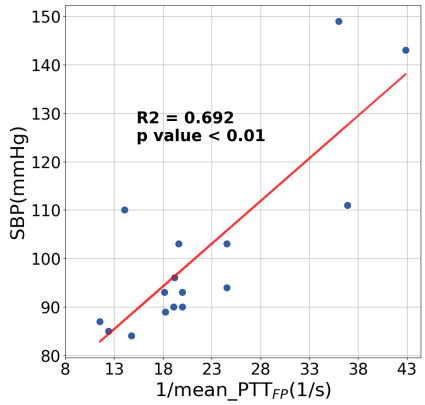

Figure 9: Linear Regression Results from Subject 4. The analysis of the inverse of $mean\_PTT_{FP}$ in relation to SBP yielded an R-squared = 0.692, with p-value <0.01, indicating a statistically significant correlation.

significant linear relationship between the inverse of $mean\_PTT_{PF}$ and the inverse of $mean\_PTT_{FP}$ with SBP.

Table 2 revealed the PTT Dominant Order information alongside R-squared values from the correlations between the inverse of $mean\_PTT_{PF}$ and the inverse of $mean\_PTT_{FP}$ with SBP. In cases where the regression model between the inverse of mean PTT and SBP was not statistically significant, the R-squared value was omitted. The highest R-squared value of 0.956 was observed for Subject 13 in the correlation between the inverse of $mean\_PTT_{PF}$ and SBP, indicating that the inverse of $mean\_PTT_{PF}$ alone explained 95.6% of the variance in estimated SBP. Among the 16 subjects, the mean and standard deviation of the R-squared values for the relationship between the inverse of $mean\_PTT_{PF}$ and SBP were

Table 1: Number of PTT Orders in 1-minute windows among 16 subjects. $DO_{PM->FH}$ represented the palm signal arrived earlier than the forehead signal consistently throughout the whole experiment, and $DO_{FH->PM}$ represented the forehead signal arrived faster than the palm signal consistently. This analysis highlighted a predominant trend of $DO_{PM->FH}$ among the 16 subjects, with a few exceptions where windows of both orders coexisted and $DO_{FH->PM}$ were observed.

Subject	PTT Dominant Order	Number of windows with $O_{PM->FH}$	Number of windows with $O_{FH->PM}$
1	$DO_{PM->FH}$	16	0
2	Both exists	11	5
3	$DO_{PM->FH}$	16	0
4	$DO_{PM->FH}$	16	0
5	$DO_{PM->FH}$	16	0
6	$DO_{PM->FH}$	16	0
7	$DO_{PM->FH}$	16	0
8	$DO_{PM->FH}$	16	0
9	$DO_{PM->FH}$	16	0
10	$DO_{FH->PM}$	0	16
11	Both exists	12	4
12	$DO_{PM->FH}$	16	0
13	Both exists	13	3
14	$DO_{PM->FH}$	16	0
15	Both exists	15	1
16	Both exists	8	8

0.81 ± 0.13. For the inverse of $mean\_PTT_{FP}$ and SBP, excluding non-significant cases, the mean R-squared value was 0.55 ± 0.16. Notably, the PTT Dominant Order consistently exhibited a higher R-squared value in the relationship between the inverse of *mean_PTT* and SBP.

Furthermore, most subjects demonstrated a PTT Dominant Order where the palm signal preceded the forehead signal ($DO_{PM->FH}$), consistent with findings reported by Lu [17]. Additionally, a common feature across all 16 subjects was the higher R-squared value observed when the mean PTT with the PTT Dominant Order was used as the independent variable. This underscored the potential significance of the PTT Dominant Order in improving the accuracy of BP estimation.

Table 2: PTT Dominant Order information of all subjects and R-squared values from the correlations of the inverse of $mean\_PTT_{PF}$ and the inverse of $mean\_PTT_{FP}$ with SBP were presented. Most of the subjects demonstrated that the inverse of mean PTT exhibited a linear relationship with SBP. Furthermore, PTT with the dominant order held higher R-squared ($1/mean\_PTT$ vs SBP) consistently.

Subject	PTT Dominant Order	R-squared ($1/mean\_PTT_{PF}$ vs SBP)	R-squared ($1/mean\_PTT_{FP}$ vs SBP)
1	$DO_{PM->FH}$	0.811	not significant
2	Both exists	0.849	0.313
3	$DO_{PM->FH}$	0.871	0.479
4	$DO_{PM->FH}$	0.874	0.692
5	$DO_{PM->FH}$	0.791	not significant
6	Both exists	0.65	0.567
7	$DO_{PM->FH}$	0.896	not significant
8	$DO_{PM->FH}$	0.896	0.394
9	$DO_{PM->FH}$	0.902	not significant
10	$DO_{FH->PM}$	0.459	0.565
11	Both exists	0.914	0.765
12	$DO_{PM->FH}$	0.854	0.253
13	Both exists	0.956	not significant
14	$DO_{PM->FH}$	0.89	0.7
15	Both exists	0.611	0.596
16	Both exists	0.719	0.724

4.3 Subgroup Analysis

A subgroup analysis was conducted by categorizing subjects into two distinct classifications: gender and exercise status. Gender was divided into male and female groups, while exercise status was categorized into pre-exercise and post-exercise groups. The analysis pursued two primary objectives: first, to determine whether there were statistically significant differences in SBP estimation error, which is the mean error across these subgroups ; second, to illustrate the hysteresis phenomenon [12], which is characterized by post-exercise SBP returning to pre-exercise levels while post-exercise HR remains elevated without immediate resetting to its initial value.

Due to the unequal sample sizes across gender groups, the Mann-Whitney U test was served as the analysis, with a p-value of 0.05 or higher considered indicative of no statistically significant difference between the groups. This analysis revealed no significant differences in SBP estimation error between both gender (U = 7742, p = 0.91) and exercise status groups (U = 9019, p = 0.16). The mean difference in SBP estimation error between females and males was

calculated to be 0.04 mmHg, while the mean difference between pre-exercise and post-exercise conditions was 0.92 mmHg. Ultimately, the results suggested that the regression performance is unlikely to be influenced by variations in gender or exercise status.

The relationship between HR and SBP was visualized in Figure 10 to further investigate the hysteresis phenomenon. This figure presented two distinct groups of measurements within the SBP range of 90 mmHg to 110 mmHg. The blue points represented pre-exercise measurements, whereas the red points denoted post-exercise measurements. In Figure 10, HR and SBP demonstrated a significant linear increase ($F = 112.34$, $p < 0.01$), with an exception observed in the highlighted red circle, which contained only red points. These red and blue points shared the same SBP range but differed in HR, providing evidence of the hysteresis phenomenon. This phenomenon occurred as the post-exercise SBP returned to its initial levels, while the HR remained elevated. In our dataset, this phenomenon was observed among 25% of the subjects.

In conclusion, there are no significant differences in SBP estimation error between various gender and exercise status groups, and a phenomenon of hysteresis can be observed among 25% of the subjects.

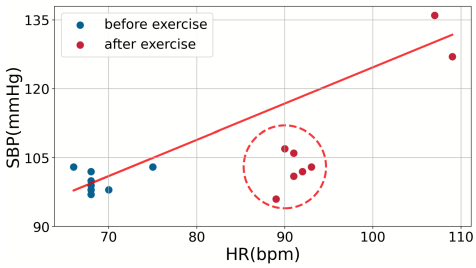

Figure 10: The plot, from Subject 2, illustrated the relationship between HR and SBP. In this graphical representation, the blue dots denoted measurements collected during the pre-exercise period, while the red dots indicated measurements recorded during the post-exercise period. HR and SBP exhibited a significant linear increase ($F = 112.34$, $p < 0.01$). However, an exception was observed within the highlighted red circle, which contained only red points, due to the hysteresis phenomenon.

5 Discussion

The results suggested that the discrepancy in PTT Order observed in this study, compared to findings reported in the literature, cannot be attributed to differences in posture, as subjects in the experiments conducted by Fan et al. [8], Secerbegovic et al. [21], and Lu et al. [17] raised their hands, which was similar to the methodology employed in this study. Therefore, the variation in PTT Order between the palm and forehead and among different subjects remains an unresolved question.

Furthermore, this study did not investigate the correlation between the inverse of mean PTT and DBP, a limitation that can be attributed to the exercise-induced BP modulation protocol. While SBP exhibited significant elevation during physical exertion, diastolic blood pressure typically demonstrated relative stability or a marginal reduction under such conditions [4, 10]. This physiological response constrained our ability to obtain sufficient DBP variability for effective regression modeling.

Nevertheless, the study provided methodological insights that suggested compelling directions for future research. Firstly, although the cohort size was limited (n = 16) and comprised predominantly Asian subjects (a factor that can restrict the applicability of the findings to a larger population), we identified considerable variations in SBP between gender groups and between different exercise statuses. These observations suggested that future studies utilizing larger and more ethnically diverse samples could confirm and extend the scope of these results. Secondly, the narrow age range of 19 to 32 years presented limitations in analyzing the effects related to age on arterial compliance. Thus, addressing this aspect in future research could substantially enhance understanding. Overall, these findings underscore the need for expanded trials that incorporate ethnically diverse populations and broader age ranges while simultaneously advocating for technological advancements in contactless BP measurement.

Calculating PTT using the palm and forehead is more complex than the M-K equation allows. The M-K equation makes simplified assumptions, presuming propagation through an infinitely long, straight, isolated cylindrical vessel, unlike the interconnected and bifurcated structures of the palm and forehead. Because of this difference, calibration is essential for future research. A promising alternative is to utilize a facial ROI combination that aligns more closely with the M-K equation, which would also eliminate the need for subjects to raise their hand.

Additionally, the phenomenon of hysteresis is observed in the relationship between HR and SBP. Despite this, it does not significantly impact the accuracy of SBP estimation using PTT, as demonstrated by a mean R-squared value of 0.81 between the inverse of mean PTT and SBP. The hysteresis phenomenon reflects that arterial stiffness and compliance are not static, which also has some impacts on PTT-SBP relationship [12]. Further investigations will focus on the implementation of non-linear models.

However, it is important to acknowledge that BP can experience substantial fluctuations following physical activity, with SBP ranges exceeding 25 mmHg within a half-hour period. These fluctuations in SBP readings reflect transient physiological changes rather than stable resting BP levels [11, 13]. This observation aligns with the standard procedure for BP measurement, which advises sitting quietly for 3 to 5 minutes without talking or moving before recording the first BP reading [15].

6 Safe and Responsible Innovation Statement

Prior to participation, subjects were provided with comprehensive study details, and their informed consent was obtained. During the experiment, subjects were informed that they might experience mild fatigue and discomfort, particularly during BP measurement. However, these sensations were minimized as the tasks were self-paced, allowing subjects to take short breaks or discontinue the experiment at their discretion. Additionally, the experimental protocol and informed consent documents received approval from the research committee. All information collected in this study will be

kept strictly confidential, anonymous and will be used solely for research and regulatory purposes.

7 Conclusion

In conclusion, this study examined the impact of the dominant order of PTT (PTT Dominant Order) between the palm and forehead on SBP estimation. Variability in the PTT Dominant Order was observed between these two sites across different subjects, but the inverse of the mean PTT extracted from both sites in PTT Dominant Order consistently showed a higher linear correlation with SBP. These findings suggested that the palm may not serve as an optimal site for such assessments. Additionally, subgroup analysis revealed no significant differences in SBP estimation error based on gender and exercise status. Furthermore, our data identified a hysteresis effect in 25% of the subjects, where SBP returned to baseline levels during post-exercise period, while HR remained consistently elevated, though this phenomenon did not significantly affect the accuracy of SBP estimation using PTT, as demonstrated by a mean R-squared value of 0.81 between the inverse of mean PTT and SBP.

Future research is encouraged to explore combinations of ROIs within the face as potential alternatives to the palm for PTT calculation and BP measurement. This approach is intended to enhance the accuracy of these assessments, facilitating advancements in contactless monitoring techniques for various applications.

References

[1] 2023. Hypertension statistics from WHO. https://www.who.int/news-room/fact-sheets/detail/hypertension.

[2] 2024. Target Heart Rates Chart. https://www.heart.org/en/healthy-living/fitness/fitness-basics/target-heart-rates.

[3] 2025. Death of cardiovascular diseases from WHO. http://who.int/health-topics/cardiovascular-diseases#tab=tab_1.

[4] Elizabeth Carpio-Rivera, José Moncada-Jiménez, Walter Salazar-Rojas, and Andrea Solera-Herrera. 2016. Acute Effects of Exercise on Blood Pressure: A Meta-Analytic Investigation. 106, 5 (2016), 422–433. doi:10.5935/abc.20160064 pmid:27168471

[5] W. Chen, T. Kobayashi, S. Ichikawa, Y. Takeuchi, and T. Togawa. 2000. Continuous Estimation of Systolic Blood Pressure Using the Pulse Arrival Time and Intermittent Calibration. 38, 5 (2000), 569–574. doi:10.1007/BF02345755

[6] Chun-Hong Cheng, Jing Wei Chin, Kwan Long Wong, Tsz Tai Chan, Hau Ching Lo, Kwan Lok Pang, Richard So, and Bryan Yan. 2025. Remote Blood Pressure Estimation from Facial Videos Using Transfer Learning: Leveraging PPG to rPPG Conversion. (2025).

[7] Felipe M. Dias, Diego A. C. Cardenas, Marcelo A. F. Toledo, Filipe A. C. Oliveira, Estela Ribeiro, Jose E. Krieger, and Marco A. Gutierrez. 2025. Exploring the limitations of blood pressure estimation using the photoplethysmography signal. 46, 4 (2025), 045007. doi:10.1088/1361-6579/adcb86 arXiv:2404.16049 [physics]

[8] Xijian Fan, Qiaolin Ye, Xubing Yang, and Sruti Das Choudhury. 2020. Robust Blood Pressure Estimation Using an RGB Camera. 11, 11 (2020), 4329–4336. doi:10.1007/s12652-018-1026-6

[9] Mohamad Kachuee, Mohammad Mahdi Kiani, Hoda Mohammadzade, and Mahdi Shabany. 2015. Cuff-Less High-Accuracy Calibration-Free Blood Pressure Estimation Using Pulse Transit Time. In *2015 IEEE International Symposium on Circuits and Systems (ISCAS)* (2015-05). 1006–1009. doi:10.1109/ISCAS.2015.7168806

[10] George A. Kelley, Kristi A. Kelley, and Zung Vu Tran. 2001. Aerobic Exercise and Resting Blood Pressure: A Meta-Analytic Review of Randomized, Controlled Trials. 4, 2 (2001), 73–80. doi:10.1111/j.1520-037X.2001.00529.x

[11] M J Kenney and D R Seals. 1993. Postexercise hypotension. Key features, mechanisms, and clinical significance. 22, 5 (1993), 653–664. doi:10.1161/01.HYP.22.5.653

[12] Qing Liu, Bryan P. Yan, Cheuk-Man Yu, Yuan-Ting Zhang, and Carmen C. Y. Poon. 2014. Attenuation of Systolic Blood Pressure and Pulse Transit Time Hysteresis During Exercise and Recovery in Cardiovascular Patients. 61, 2 (2014), 346–352. doi:10.1109/TBME.2013.2286998

[13] J. D. MacDougall, D. Tuxen, D. G. Sale, J. R. Moroz, and J. R. Sutton. 1985. Arterial blood pressure response to heavy resistance exercise. 58, 3 (1985), 785–790. doi:10.1152/jappl.1985.58.3.785

[14] Ping-Kwan Man, Kit-Leong Cheung, Nawapon Sangsiri, Wilfred Jin Shek, Kwan-Long Wong, Jing-Wei Chin, Tsz-Tai Chan, and Richard Hau-Yue So. 2022. Blood Pressure Measurement: From Cuff-Based to Contactless Monitoring. 10, 10 (2022), 2113. doi:10.3390/healthcare10102113

[15] Paul Muntner, Daichi Shimbo, Robert M. Carey, Jeanne B. Charleston, Trudy Gaillard, Sanjay Misra, Martin G. Myers, Gbenga Ogedegbe, Joseph E. Schwartz, Raymond R. Townsend, Elaine M. Urbina, Anthony J. Viera, William B. White, Jackson T. Wright, and on behalf of the American Heart Association Council on Hypertension; Council on Cardiovascular Disease in the Young; Council on Cardiovascular and Stroke Nursing; Council on Cardiovascular Radiology and Intervention; Council on Clinical Cardiology; and Council on Quality of Care and Outcomes Research. 2019. Measurement of Blood Pressure in Humans: A Scientific Statement From the American Heart Association. 73, 5 (2019). doi:10.1161/HYP.0000000000000087

[16] Kenta Murakami, Mototaka Yoshioka, and Jun Ozawa. 2015. Non-Contact Pulse Transit Time Measurement Using Imaging Camera, and Its Relation to Blood Pressure. In *2015 14th IAPR International Conference on Machine Vision Applications (MVA)* (2015-05). 414–417. doi:10.1109/MVA.2015.7153099

[17] Lu Niu, Jeremy Speth, Nathan Vance, Ben Sporrer, Adam Czajka, and Patrick Flynn. 2023. Full-Body Cardiovascular Sensing with Remote Photoplethysmography. In *2023 IEEE/CVF Conference on Computer Vision and Pattern Recognition Workshops (CVPRW)* (Vancouver, BC, Canada, 2023-06). IEEE, 5994–6004. doi:10.1109/CVPRW59228.2023.00638

[18] Omkar R. Patil, Wei Wang, Yang Gao, and Zhanpeng Jin. 2019. A Camera-Based Pulse Transit Time Estimation Approach Towards Non-Intrusive Blood Pressure Monitoring. In *2019 IEEE International Conference on Healthcare Informatics (ICHI)* (2019-06). 1–10. doi:10.1109/ICHI.2019.8904498

[19] C.C.Y. Poon and Y.T. Zhang. 2005. Cuff-Less and Noninvasive Measurements of Arterial Blood Pressure by Pulse Transit Time. In *2005 IEEE Engineering in Medicine and Biology 27th Annual Conference* (Shanghai, China, 2005). IEEE, 5877–5880. doi:10.1109/IEMBS.2005.1615827

[20] Meng Rong and Kaiyang Li. 2021. A Blood Pressure Prediction Method Based on Imaging Photoplethysmography in Combination with Machine Learning. 64 (2021), 102328. doi:10.1016/j.bspc.2020.102328

[21] A. Secerbegovic, J. Bergsland, P.S. Halvorsen, N. Suljanovic, A. Mujcic, and I. Balasingham. 2016. Blood Pressure Estimation Using Video Plethysmography. In *2016 IEEE 13th International Symposium on Biomedical Imaging (ISBI)* (2016-04). 461–464. doi:10.1109/ISBI.2016.7493307

[22] Thomas Stogiannopoulos and Nikolaos Mitianoudis. 2024. Non-Contact Blood Pressure Estimation Using Forehead and Palm Infrared Video. 4, 1 (2024), 437–453. Issue 1. doi:10.3390/biomedinformatics4010025

[23] Toshiyo Tamura, Yuka Maeda, Masaki Sekine, and Masaki Yoshida. 2014. Wearable Photoplethysmographic Sensors—Past and Present. 3, 2 (2014), 282–302. Issue 2. doi:10.3390/electronics3020282

[24] Hirofumi Tanaka, Kevin D Monahan, and Douglas R Seals. 2001. Age-Predicted Maximal Heart Rate Revisited. 37, 1 (2001), 153–156. doi:10.1016/S0735-1097(00)01054-8

[25] Wim Verkruysse, Lars O. Svaasand, and J. Stuart Nelson. 2008. Remote Plethysmographic Imaging Using Ambient Light. 16, 26 (2008), 21434–21445. doi:10.1364/OE.16.021434

[26] Charalambos Vlachopoulos, Michael O'Rourke, and Wilmer W Nichols. 2011. *McDonald's blood flow in arteries* (6 ed.). Hodder Arnold, London, England.

[27] Bing-Fei Wu, Bing-Jhang Wu, Bing-Ruei Tsai, and Chi-Po Hsu. 2022. A Facial-Image-Based Blood Pressure Measurement System Without Calibration. 71 (2022), 1–13. doi:10.1109/TIM.2022.3165827

[28] Carolin Wuerich, Robin Rademacher, Christian Wiede, and Anton Grabmaier. 2021. PTT-Based Contact-Less Blood Pressure Measurement Using an RGB-Camera. 7, 2 (2021), 375–378. doi:10.1515/cdbme-2021-2095